HHS Public Access

Author manuscript

Gene Ther. Author manuscript; available in PMC 2017 October 25.

Published in final edited form as:

Gene Ther. 2017 June ; 24(6): 361–369. doi:10.1038/gt.2017.27.

Improved Gene Delivery to Adult Mouse Spinal Cord Through the Use of Engineered Hybrid Adeno-Associated Viral serotypes

Jason J. Siu[1,2,3], **Nicholas J. Queen**[1], **Wei Huang**[1], **Feng Qin Yin**[2], **Xianglan Liu**[1], **Dana M. McTigue**[2], and **Lei Cao**[1,2]

[1]Department of Cancer Biology and Genetics, The Ohio State University, Columbus, OH 43210

[2]Neuroscience Graduate Program, The Ohio State University, Columbus, OH 43210

[3]Medical Scientist Training Program, The Ohio State University, Columbus, OH 43210

Abstract

Adeno-associated viral (AAV) vectors are often used in gene therapy for neurological disorders because of its safety profile and promising results in clinical trials. One challenge to AAV gene therapy is effective transduction of large numbers of the appropriate cell type, which can be overcome by modulating the viral capsid through DNA shuffling. Our previous study demonstrates that Rec2, among a family of novel engineered hybrid capsid serotypes (Rec1~4) transduces adipose tissue with far superior efficiency than naturally occurring AAV serotypes. Here we assessed the transduction of adult spinal cord at two different doses of AAV vectors expressing green fluorescent protein (2×10^9 or 4×10^8 viral particles) via intraparenchymal injection at the thoracic vertebral level T9. In comparison to an equal dose of the currently preferable AAV9 serotype, Rec3 serotype transduced a broader region of spinal cord up to approximately 1.5 cm longitudinally, and displayed higher transgene expression and increased maximal transduction rates of astrocytes at either dose and neurons at the lower dose. These novel engineered hybrid vectors could provide powerful tools at lower production costs to manipulate gene expression in spinal cord for mechanistic studies, or provide potent vehicles for gene therapy delivery, such as neurotrophins, to spinal cord.

Introduction

Recombinant AAV (rAAV) vectors are not only powerful vehicles of gene delivery for basic research but also have been widely used for gene therapy in genetic and acquired diseases (1). rAAV vectors have become the preferred *in vivo* gene delivery system because of their characteristics including broad tropism of both dividing and postmitotic tissues, high efficiency of gene transfer, long-lasting transgene expression, low immunogenicity, and minimal toxicity (2). For application in the central nervous system (CNS), extensive

Correspondence should be addressed to: L.C., Columbus, OH USA. 910 BRT, 460 W. 12th Ave., Columbus, OH 43210, Telephone: 614-3665679, Fax: 614-2474905, lei.cao@osumc.edu.

Conflict of interest

The authors declare no conflict of interest.

investigations have been made to characterize an optimal rAAV serotype for specific needs: global versus focal transduction, tropism for different cell types within the CNS (neurons, astrocytes and oligodendrocytes), and route of administration, such as intraparenchymal stereotactic injection, intracerebroventricular injection to allow circulation throughout the cerebrospinal fluid (CSF), and systemic delivery by intravenous injection (2). Furthermore, engineered serotypes via rational and combinatorial approaches are generated to overcome limitations of naturally occurring serotypes, improve gene transfer efficacy, and avoid immune reactions (3). For example, novel hybrid AAV capsid serotypes: Rec1, 2, 3, and 4 were generated by shuffling the fragments of capsid sequences that matched in all three non-human primate AAV serotypes cy5, rh20, and rh39, with AAV8 (4). We recently evaluated the transduction efficacy of these engineered serotypes in adipose tissues that are difficult to be transduced by naturally occurring AAV serotypes (5–7). Rec2 vector leads to high transduction of adipose tissue, superior to naturally occurring serotypes (AAV1, AAV8, and AAV9) as well as other engineered serotypes (Rec1, Rec3, Rec4) (8). Rec2 vector is particularly efficient for gene delivery to brown adipose tissue, even at a dose that is at least 1–2 orders lower than the naturally occurring serotypes (8). Here we further study the tropisms of these engineered serotypes and explore their application in the spinal cord. Up to date AAV9 has become the most preferable serotype for spinal cord gene transfer (9–14). Therefore, we characterized the gene delivery of the series of engineered serotypes (Rec2, Rec3, Rec4) and compared with AAV9 by intraparenchymal injection to the spinal cord of adult mice.

Results

Vector diffusion within spinal cord

Adult mice were randomized to receive a single dose of Rec2, Rec3, Rec4, or AAV9 vectors carrying GFP at the T9 vertebral level (2×10^9 vg AAV per mouse). GFP fluorescence was examined three weeks post-injection (Fig 1a). The longitudinal transduction range was defined as the observance of GFP^+ cell bodies (Fig 1c). Among the serotypes tested, Rec3 showed the most diffusion with its transduction as far as 1.45 ± 0.07 cm of spinal cord whereas Rec2 showed more focal transduction (0.59 ± 0.11 cm) (Fig 1b). On the other hand, AAV9 transduced 1.21 ± 0.18 cm, similar to the transduction range of Rec4 serotype (1.09 ± 0.12 cm).

Intensity of transgene expression

We next determined whether transgene expression was greater with the Rec vectors through quantification of fluorescence intensity on the ipsilateral as well as contralateral non-injected side of spinal cord relative to injection site (Fig 2a, b). The section with the most intense GFP fluorescence from each spinal cord was selected, and the fluorescence was measured. The average fluorescence intensity of Rec3 was significantly greater on both ipsilateral (1.7-fold) and contralateral (2.0-fold) spinal cord than AAV9 (Fig 2c, d). Assessing the sum fluorescence intensity of both sides of spinal cord, Rec3 was still significantly 1.8-fold higher than AAV9 (Fig 2c), whereas no significant difference in GFP intensity was observed between AAV9, Rec2, and Rec4.

Cellular tropism

We characterized the cell types transduced by the series of AAV vectors through immunohistochemistry colocalization with neuronal marker NeuN (Fig 3a). On the ipsilateral injection side, a trend towards higher transduction of $NeuN^+$ neurons was observed in both Rec2 and Rec3 (88.07% and 87.96%, respectively) compared to that by AAV9 (73.20%) (Fig 3b). In addition, Rec3 and Rec4 also led to a trend of greater $NeuN^+$ neuronal transduction than AAV9 (Rec3: 87.80%, Rec4: 72.02%, AAV9: 63.84%) on the contralateral non-injected side (Fig 3b). Summating the total number of GFP^+ neurons, all three Rec vectors resulted in higher- though not significant- transduction rates of neurons than AAV9 (Fig 3c).

Astrocyte transduction was quantified using the marker glial fibrillary acidic protein (GFAP, Fig 4a). Both Rec3 and Rec4 showed increased transduction rates of $GFAP^+$ astrocytes compared to AAV9 (86.66% and 80.93% versus 63.43%, respectively; Fig 4b) on the ipsilateral injection side. Furthermore, Rec3 also transduced more $GFAP^+$ astrocytes than AAV9 on the contralateral non-injected side (86.10% versus 54.85%, respectively, Fig 4b). Rec3 and Rec4 vectors resulted in higher astrocyte transduction rates than AAV9 when totaling the GFP^+GFAP^+ astrocytes bilaterally (Fig 4c).

Diffusion of transgene product

Lastly, we investigated the distribution of transgene product throughout the CNS when the AAV vectors were injected intraparenchymally at the T9 level of spinal cord (Fig 5a). GFP fluorescence was observed as far as the rostral spinal cord (Fig 5ab) and caudal or lumbosacral spinal cord (Fig 5a, c), essentially the entire spinal cord. Through qualitative observations, Rec3 showed the highest number of GFP^+ fibers throughout the spinal cord than the other serotypes (Fig 5b, c). No substantial GFP^+ cell bodies were found in the brain. However, GFP^+ axonal fibers were observed in both cerebellum and brainstem for all AAV serotypes (Fig 6).

Vector properties at a lower dose

With the Rec3 serotype displaying the most diffusion, greatest fluorescence intensity, and a trend towards transducing more neurons and astrocytes than AAV9, we next wondered whether this pattern would hold at a different viral dose. Thus, the same intraparenchymal injections were performed on adult mice, who received either Rec3 or AAV9 vectors carrying GFP at a dose of 4×10^8 vg. At this 5-fold lower dose, GFP^+ cell bodies were observed across three sections for Rec3 versus two for AAV9 (Fig 7a). Rec3 diffusion across spinal cord was 1.22 ± 0.07 cm while AAV9 transduced 0.98 ± 0.03 cm (Fig 7b). Regarding average fluorescence intensity, Rec3 was significantly greater than AAV9 by 1.5-fold, whether on ipsilateral (1.46-fold), contralateral (1.48-fold), or entire spinal cord (1.47-fold) (Fig 7c, d). Next, quantification of $NeuN^+$ neurons and $GFAP^+$ astrocytes transduced (Fig 8a, d) revealed that ipsilaterally, a significantly larger percentage of $NeuN^+$ neurons was transduced by Rec3 compared to AAV9 (92.37% vs. 79.80%, respectively) (Fig 8b). In addition, Rec3 significantly transduced higher rates of $NeuN^+$ neurons than AAV9 (81.15% vs. 72.04%, respectively) on the contralateral non-injected side. Summating the total number of GFP^+ neurons, Rec3 resulted in significantly higher transduction rates of neurons than

AAV9 (Fig 8c). Similarly, astrocyte transduction for Rec3 was significantly greater on the ipsilateral injection side compared to AAV9 (82.28% vs. 75.17%, respectively, Fig 8e). Contralalerally, however, $GFAP^+$ astrocyte transduction was higher for Rec3 albeit insignificant when compared to AAV9 (73.10% versus 70.93%, respectively). Lastly, Rec3 vector resulted in higher astrocyte transduction rates than AAV9 when totaling the GFP^+GFAP^+ astrocytes bilaterally (Fig 8f).

Discussion

The goal of this study was to determine whether the newly engineered hybrid serotypes of rAAV harbored desirable properties for gene transfer to the spinal cord. Among the naturally occurring serotypes that have been examined for intraparenchymal injection to the spinal cord of adult rodents, AAV9 displays the highest transduction efficiency and widest distribution (10, 14). Thus, we compared the efficacy of a single thoracic intraparenchymal injection of Rec2, Rec3, and Rec4 serotypes with AAV9. Overall, Rec3 showed the highest transduction efficiency among the serotypes tested including AAV9. The longitudinal diffusion of GFP-expressing cell bodies in Rec3 vector injected mice reached approximately 1.5 cm, covering a large portion of the thoracic and lumbar spinal cord. Snyder, *et al.*, reports that intraparenchymal injection of AAV9 (6.25×10^8 vg per injection) results in less than 5 mm longitudinal diffusion, which is better than that of AAV1, AAV6 and AAV8 (10). While the doses we used in this study were higher (2×10^9 vg) and lower (4×10^8 vg) than that of Synder, *et al.*, the longitudinal range of transgene-expressing cell bodies of Rec3 serotype was still significantly increased compared to AAV9 at both high and low dosages tested. Furthermore, the longitudinal transduction range of intraparenchymal Rec3 (2×10^9 vg) was at least two-fold farther than the intrathecal injection of AAV9 (2.5×10^9 vg) using the same promoter, the chicken β–actin promoter with CMV enhancer (10). Moreover, Rec3 demonstrated higher transduction on the contralateral non-injected side of spinal cord than all the serotypes tested. Overall, Rec3 provided the most widespread transduction while Rec2 displayed the most focal transduction.

Quantification of the GFP fluorescence intensity showed that Rec3 led to the highest maximal transgene protein on both the ipsilateral injected and contralateral non-injected side of spinal cord, regardless of the doses tested. This could be due to a higher density of transduction (more cells being transduced), higher transgene expression within the transduced cells, or a combination of both. Interestingly, Rec2 serotype is highly efficient at transducing adipose tissues while Rec3, Rec4, and AAV9 perform poorly (8, 15). The ability of these recombinant serotypes to transduce different tissues may be concerning when tissue specificity is preferred. However, focal, localized transduction within a tissue or specific tissue type is achievable by a combination of approaches including limiting dose, direct injection to the targeting tissue, using a tissue-specific promoter, and incorporating microRNA targeting sequences (for example, miR-122 targeting sequence to restrict transgene expression in liver (15)). The distinct tissue tropism of these engineered serotypes provides an example that engineering naturally occurring serotypes is a useful approach to expand the current AAV vector toolkit for both basic and translational applications. In diseases such as spinal cord injury, where injury may be focal, utilizing a vector with localized transduction such as Rec2 could be ideal. On the other hand, for diseases requiring

widespread transduction, Rec3 vector, which leads to broader transduction and higher transgene expression, may be economically advantageous for the clinic, whereas lower doses, and therefore less viral vector production, would be required to produce an effect equivalent to AAV9.

The engineered serotypes as well as AAV9 transduced both neurons and astrocytes in the adult spinal cord. When analyzing regions around the dorsal and ventral horns, all Rec vectors significantly enhanced the maximal transduction rate of astrocytes compared to AAV9 at the dose of 2×10^9 vg per mouse. Rec3 was particularly efficient, leading to approximately 86% transduction of the total $GFAP^+$ astrocytes while AAV9 showed approximately 63%. At the 5-fold lower dose, the transduction of neurons and astrocytes by Rec3 is significantly more pronounced relative to AAV9. This could quite possibly be due to the larger transduction volume and/or better detection of colocalized cells due to increased transgene fluorescence. Future 3D imaging studies of whole spinal cord, beyond the regions near the dorsal and motor horns, would confirm or improve the characterization of these results. A recent study reports that a single intrathecal injection of rhesus-10 AAV serotype (rAAVrh10) into the lumbar cistern can transduce 60 to 90% of the cells in the spinal cord at a dose of 4×10^{10} vg per mouse. In addition, the transgene is expressed in all cell types including neurons, glial, ependymal cells, and endothelial cells in the spinal cord. Furthermore, transgene expression is detected in some brain areas as far as the frontal cortex and olfactory bulbs (16). In this study, no GFP^+ cell bodies were observed in the brain when the Rec vectors were injected intraparenchymally into the spinal cord at a dose of 2×10^9 vg per mouse although GFP fluorescence was found in brainstem and cerebellum, suggesting retrograde transport of transgene protein. It will be interesting to examine the transduction efficiency, cell tropism, and potential distribution to the broad CNS of these engineered serotypes- particularly Rec3- via intrathecal or other systemic delivery methods such as intravenous injection (17–21).

In summary, the novel engineered Rec serotypes- and particularly Rec3- were highly efficient in transducing the mature mouse spinal cord via intraparenchymal injection. The Rec3 serotype specifically led to the most widespread transduction, highest transgene expression, and the most maximal transduction rate of both neurons and astrocytes among all the serotypes examined including the widely used and clinically approved AAV9 (*Gene Transfer Clinical Trial for Spinal Muscular Atrophy Type 1.* https://clinicaltrials.gov/ct2/show/NCT02122952) (22, 23). These engineered serotypes provide vehicles for genetic manipulations of spinal cord for basic research, disease modeling, and potential gene therapy for diseases affecting entire the spinal cord, such as spinal muscular atrophy and amyotrophic lateral sclerosis.

Materials & Methods

rAAV vector construction and packaging

The recombinant AAV capsid serotypes (Rec1-4) were generated by shuffling the fragments of capsid sequences that matched in all three nonhuman primate AAV serotypes (cy5, rh20, rh39) and AAV8. The three new recombinant serotypes previously identified, with greater transduction efficiency than rAAV8, cy5, rh20, and rh39, were originally supplied by

Guangping Gao and the Gene Therapy Program Vector Core, Department of Medicine, University of Pennsylvania, where further details of the identification of these sequences is available. The details of Rec1-4 serotypes are described before (4). To generate hybrid AAV vectors, GFP was cloned into an AAV expression plasmid under the control of the chicken β-actin promoter plus cytomegalovirus enhancer and containing woodchuck hepatitis virus post-transcriptional regulatory element (WPRE), and bovine growth hormone (bGH) polyadenylation signal flanked by AAV2 inverted terminal repeats. Human embryonic kidney 293 cells were co-transfected with three plasmids—AAV plasmid, appropriate helper plasmid encoding *rep* and *cap* (Rec1-4) genes or AAV9, and adenoviral helper pFΔ6—using standard calcium phosphate transfection. rAAV vectors were purified from the cell lysate by ultracentrifugation through an iodixanol density gradient. Vectors were titered using real-time quantitative PCR (qPCR, ABI StepOnePlus; Applied Biosystems, Foster City, CA) and adjusted to 2×10^{13} viral genomic particles (vg) per mL 0.01% pluronic F-68 in phosphate buffered saline (PBS) for stereotaxic injections. Two different batches of vector per serotype were used in this study.

Mice

Male C57BL/6 mice, 9 weeks of age were purchased from Charles River Laboratories, Wilmington, MA. Animals were housed in groups of no more than five per cage in a 12:12 light:dark cycle with *ad libitum* access to standard rodent chow and water in a temperature- and humidity-controlled environment. All mice experiments were carried out in compliance with the regulations of the Ohio State University Institutional Animal Care and Use Committee.

Stereotaxic surgery

Surgeries were performed in collaboration with The Ohio State Neuroscience Center Injury and Behavior Core. Adult male mice were randomized to receive AAV serotype vectors. Mice anesthetized with a single dose of 100 mg/kg ketamine and 20 mg/kg xylazine. Laminectomy was then performed to expose spinal cord at the T9 vertebral level. Mice then received one unilateral right-side injection of high (2×10^9 vg) or low (4×10^8 vg) dose AAV in 1.0 μL (ML: 0.5, DV: −0.8) at the grey-white matter junction, according to the Spinal Cord Atlas (Watson, Paxinos, and Kayalioglu, 2009), with a pulled glass micropipette and air-pressurized nanoinjector. Afterwards, muscles were sutured overlying the spinal cord and skin was sealed with surgical clips. All animals were administered 2 mL saline in heated recovery cages post-surgery, and after waking and ambulating were returned to standard cages and monitored weekly until sacrifice three weeks later.

Tissue preparation

Mice were intracardially perfused with 4% paraformaldehyde (PFA, Sigma, St. Louis, MO) in PBS, and fixed spinal cords were placed in 4% PFA overnight. The following day, spinal cords were washed in PBS three times before being immersed in 30% sucrose in PBS for at least three days. Spinal cords were then divided into eight 0.5 cm segments and frozen in O.C.T. (Sakura Finetek, Torrance, CA) before being sectioned into 30 μm slices on a Leica cryostat.

Immunohistochemistry and imaging

Slides with cryosections were dried, washed in PBS, and blocked in 5% normal goat serum, 1% bovine serum albumin, 0.3% Triton TX-100, 0.3M glycine, and 0.03% sodium azide in PBS for one hour. Also in blocking buffer, primary antibodies included mouse anti-NeuN (Chemicon, Cat. No. MAB377, 1:500, Darmstadt, Germany) or mouse anti-GFAP (Millipore, Cat. No. MAB3402, 1:500, Darmstadt, Germany), and were applied onto tissue overnight at 4 °C. The following day, slides were washed three times in PBS before incubation with appropriate AlexaFluor secondary antibodies (Invitrogen, Carlsbad, CA) and nuclear counterstain DAPI in blocking buffer at room temperature for one hour. After three washes in PBS, slides were mounted using Aqua-Poly/Mount (Polysciences, Warrington, PA) and coverslipped. Confocal microscopy was performed on a FluoView FV1000 microscope (Zeiss, Oberkochen, Germany).

Quantification of images

Regarding diffusion, images were captured at 2.5x or 10x magnification. The longitudinal diffusion of GFP was determined by counting the number of sections (in one of each series of eight 30 μm sections) that had GFP expression in cell bodies and then multiplying them by 0.5 cm, the approximate distance between consecutive adjacent sections (i.e., 3 sections × 0.5 cm between sections in each series). Each mouse spinal cord was sectioned into 15 series/rows on 1 slide. From all 5 mice injected per serotype, the values of all series were summed and averaged. This estimate was calculated for each serotype and used to compare diffusion distance between serotypes.

GFP fluorescence intensity was quantified using ImageJ/Fiji (NIH, Bethesda, MD). The most fluorescent coronal section from each serotype (n=5 mice per serotype) was acquired. Random rectangular selections of equal height and width (or pixel area) were drawn for both ipsilateral and contralateral spinal cord across all samples. Six random areas were selected in the dorsal as well as ventral sections of both the ipsilateral and contralateral sides of injection. Quantification of colocalized cells was also analyzed with the same method, and measurements from the ipsilateral or contralateral side were summated and analyzed with statistical software (below).

Statistical analysis

Values are expressed as mean ± SEM. Normal distribution was confirmed and *t*-test (low dose comparisons, 2 samples) or one-way ANOVA with Dunnett's multiple comparisons test (high dose comparisons, 4 samples) was used to assess for significant differences with Prism Mac version 6.0f software (GraphPad, La Jolla, CA).

Acknowledgments

This work was supported by NIH grants CA163640, CA166590, and AG041250 (to L. Cao), and P30 NS045758 (to The Ohio State Neuroscience Center Injury and Behavior Core).

References

1. Kotterman MA, Schaffer DV. Engineering adeno-associated viruses for clinical gene therapy. Nature reviews Genetics. 2014; 15(7):445–51.
2. Mingozzi F, High KA. Therapeutic in vivo gene transfer for genetic disease using AAV: progress and challenges. Nature reviews Genetics. 2011; 12(5):341–55.
3. Asokan A, Schaffer DV, Samulski RJ. The AAV vector toolkit: poised at the clinical crossroads. Mol Ther. 2012; 20(4):699–708.
4. Charbel Issa P, De Silva SR, Lipinski DM, Singh MS, Mouravlev A, You Q, et al. Assessment of tropism and effectiveness of new primate-derived hybrid recombinant AAV serotypes in the mouse and primate retina. PloS one. 2013; 8(4):e60361. [PubMed: 23593201]
5. Mizukami H, Mimuro J, Ogura T, Okada T, Urabe M, Kume A, et al. Adipose tissue as a novel target for in vivo gene transfer by adeno-associated viral vectors. Human gene therapy. 2006; 17(9): 921–8. [PubMed: 16972760]
6. Zhang FL, Jia SQ, Zheng SP, Ding W. Celastrol enhances AAV1-mediated gene expression in mice adipose tissues. Gene therapy. 2011; 18(2):128–34. [PubMed: 20844567]
7. Jimenez V, Munoz S, Casana E, Mallol C, Elias I, Jambrina C, et al. In vivo adeno-associated viral vector-mediated genetic engineering of white and brown adipose tissue in adult mice. Diabetes. 2013; 62(12):4012–22. [PubMed: 24043756]
8. Liu X, Magee D, Wang C, McMurphy T, Slater A, During M, et al. Adipose tissue insulin receptor knockdown via a new primate-derived hybrid recombinant AAV serotype. Molecular therapy Methods & clinical development. 2014:1. [PubMed: 26015941]
9. Foust KD, Nurre E, Montgomery CL, Hernandez A, Chan CM, Kaspar BK. Intravascular AAV9 preferentially targets neonatal neurons and adult astrocytes. Nat Biotechnol. 2009; 27(1):59–65. [PubMed: 19098898]
10. Snyder BR, Gray SJ, Quach ET, Huang JW, Leung CH, Samulski RJ, et al. Comparison of adeno-associated viral vector serotypes for spinal cord and motor neuron gene delivery. Human gene therapy. 2011; 22(9):1129–35. [PubMed: 21443428]
11. Foust KD, Wang X, McGovern VL, Braun L, Bevan AK, Haidet AM, et al. Rescue of the spinal muscular atrophy phenotype in a mouse model by early postnatal delivery of SMN. Nat Biotechnol. 2010; 28(3):271–4. [PubMed: 20190738]
12. Gray SJ, Matagne V, Bachaboina L, Yadav S, Ojeda SR, Samulski RJ. Preclinical differences of intravascular AAV9 delivery to neurons and glia: a comparative study of adult mice and nonhuman primates. Mol Ther. 2011; 19(6):1058–69. [PubMed: 21487395]
13. Dayton RD, Wang DB, Klein RL. The advent of AAV9 expands applications for brain and spinal cord gene delivery. Expert Opin Biol Ther. 2012; 12(6):757–66. [PubMed: 22519910]
14. Burger C, Gorbatyuk OS, Velardo MJ, Peden CS, Williams P, Zolotukhin S, et al. Recombinant AAV viral vectors pseudotyped with viral capsids from serotypes 1, 2, and 5 display differential efficiency and cell tropism after delivery to different regions of the central nervous system. Mol Ther. 2004; 10(2):302–17. [PubMed: 15294177]
15. Huang W, McMurphy T, Liu X, Wang C, Cao L. Genetic Manipulation of Brown Fat Via Oral Administration of an Engineered Recombinant Adeno-associated Viral Serotype Vector. Mol Ther. 2016; 24(6):1062–9. [PubMed: 26857843]
16. Guo Y, Wang D, Qiao T, Yang C, Su Q, Gao G, et al. A Single Injection of Recombinant Adeno-Associated Virus into the Lumbar Cistern Delivers Transgene Expression Throughout the Whole Spinal Cord. Mol Neurobiol. 2015
17. Wang H, Yang B, Qiu L, Yang C, Kramer J, Su Q, et al. Widespread spinal cord transduction by intrathecal injection of rAAV delivers efficacious RNAi therapy for amyotrophic lateral sclerosis. Hum Mol Genet. 2014; 23(3):668–81. [PubMed: 24108104]
18. Hordeaux J, Dubreil L, Deniaud J, Iacobelli F, Moreau S, Ledevin M, et al. Efficient central nervous system AAVrh10-mediated intrathecal gene transfer in adult and neonate rats. Gene therapy. 2015; 22(4):316–24. [PubMed: 25588740]

19. Schuster DJ, Dykstra JA, Riedl MS, Kitto KF, Belur LR, McIvor RS, et al. Biodistribution of adeno-associated virus serotype 9 (AAV9) vector after intrathecal and intravenous delivery in mouse. Front Neuroanat. 2014; 8:42. [PubMed: 24959122]

20. Duque S, Joussemet B, Riviere C, Marais T, Dubreil L, Douar AM, et al. Intravenous administration of self-complementary AAV9 enables transgene delivery to adult motor neurons. Mol Ther. 2009; 17(7):1187–96. [PubMed: 19367261]

21. Yang B, Li S, Wang H, Guo Y, Gessler DJ, Cao C, et al. Global CNS transduction of adult mice by intravenously delivered rAAVrh.8 and rAAVrh.10 and nonhuman primates by rAAVrh.10. Mol Ther. 2014; 22(7):1299–309. [PubMed: 24781136]

22. Valori CF, Ning K, Wyles M, Mead RJ, Grierson AJ, Shaw PJ, et al. Systemic delivery of scAAV9 expressing SMN prolongs survival in a model of spinal muscular atrophy. Sci Transl Med. 2010; 2(35):35ra42.

23. Meyer K, Ferraiuolo L, Schmelzer L, Braun L, McGovern V, Likhite S, et al. Improving single injection CSF delivery of AAV9-mediated gene therapy for SMA: a dose-response study in mice and nonhuman primates. Mol Ther. 2015; 23(3):477–87. [PubMed: 25358252]

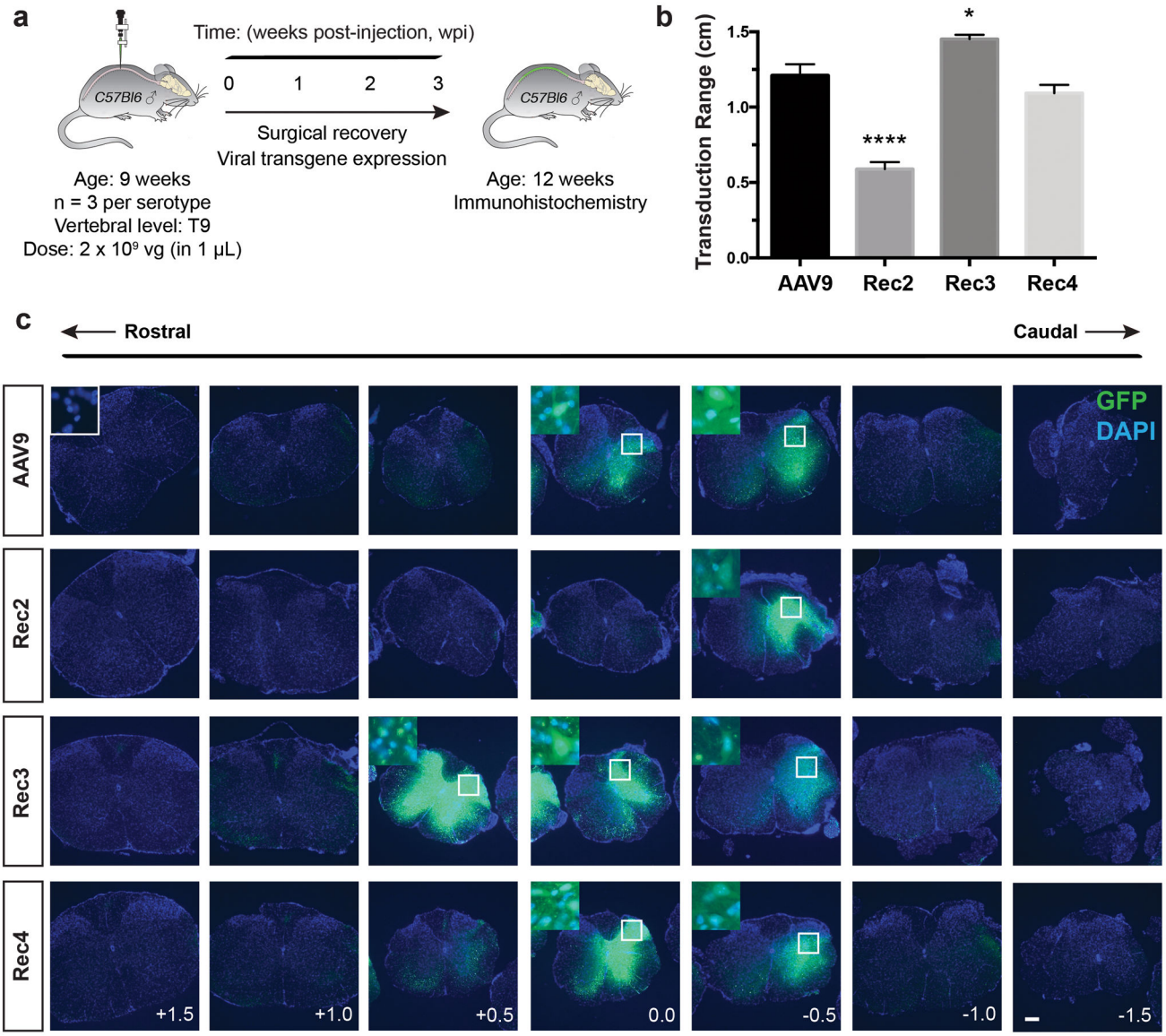

Figure 1. Methods and longitudinal transduction range of Rec serotypes compared to AAV9

(a) Experimental design. Groups of 9-week-old C57BL6 mice (n=5) were stereotaxically injected with an AAV serotype (AAV9, Rec2-4) containing *CBA*-GFP at vertebral level T9 into the gray-white matter junction. 3 weeks post-injection (wpi), animals were perfused for immunohistochemical analysis. **(b)** Quantification of longitudinal transduction in cm by the various AAV serotypes. **(c)** Representative images of GFP transgene expression along the spinal cord. +/− indicates distance in cm away from the injection site (vertebral level T9). n=5 mice per vector. Error bars = S.E.M. * $p < 0.05$. **** $p < 0.0001$. Scale bar = 200 µm.

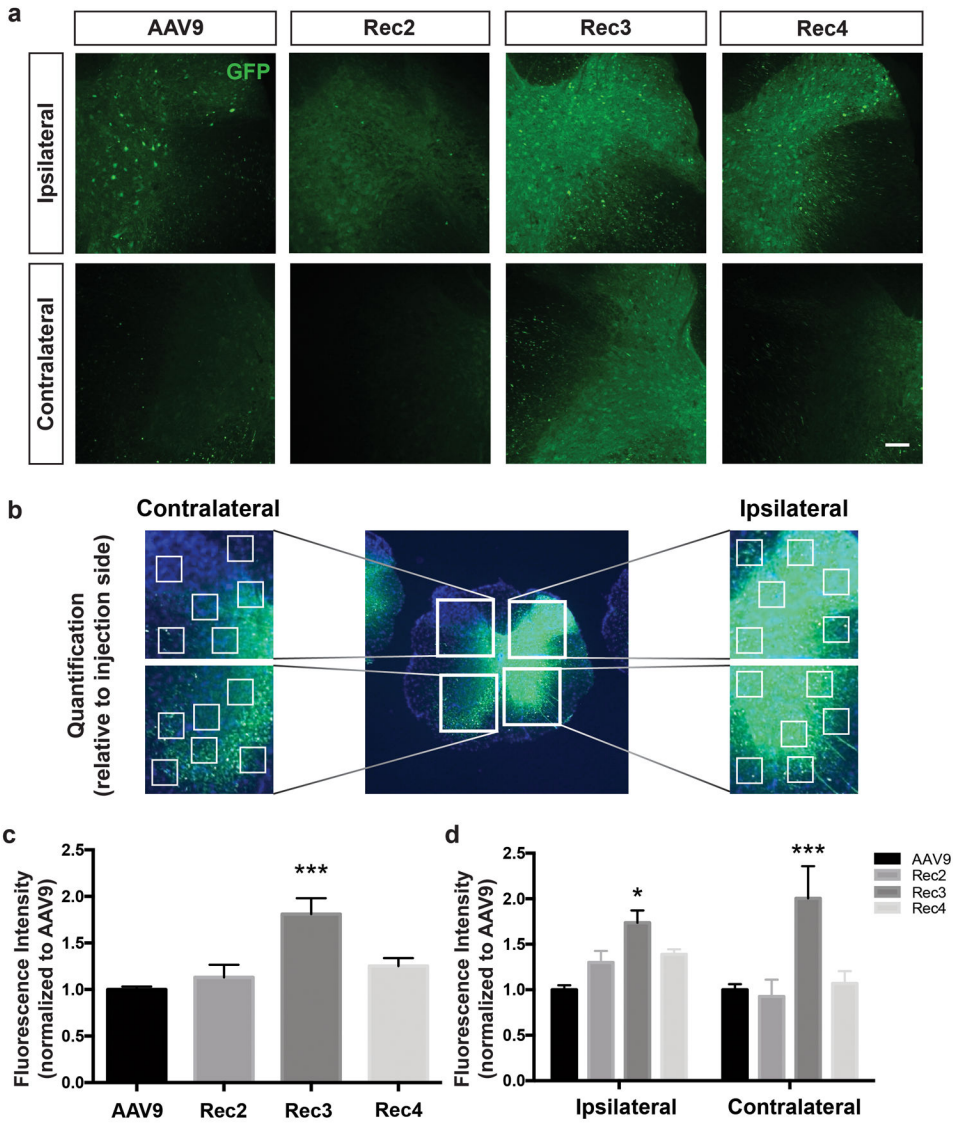

Figure 2. Transgene expression of Rec serotypes vs. AAV9 as measured by GFP intensity

(a) Representative images of sections quantified. **(b)** Example of methodology applied to quantify GFP intensity in a random, unbiased manner. **(c)** Quantification of total GFP intensity across whole slice. **(d)** Quantification of GFP intensity ipsilateral and contralateral to side of injection. n=5 mice per vector. n=12 random quadrants per side. Error bars = S.E.M. * = $p < 0.05$. *** $p < 0.001$. Scale bar = 100 μm.

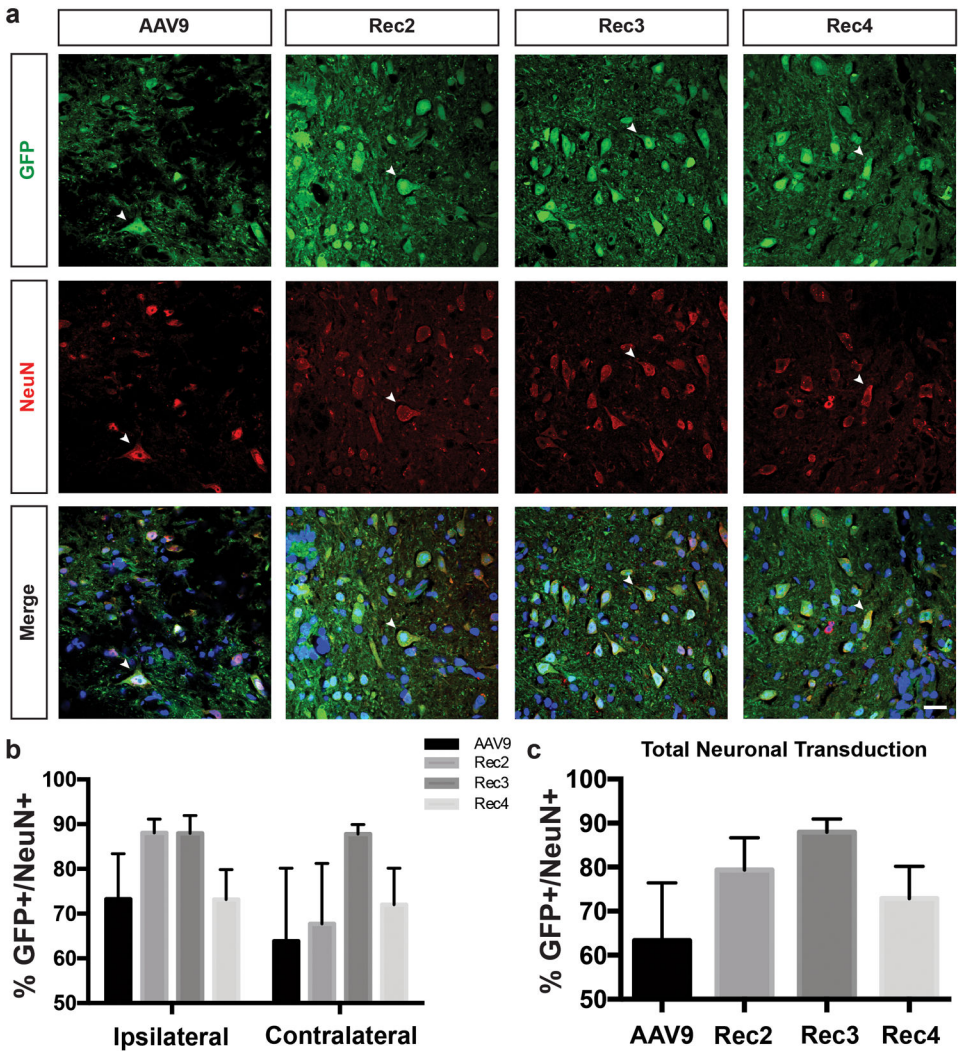

Figure 3. Comparison of neuronal transduction by Rec vectors vs. AAV9

(a) Transduction (GFP, green) of neurons assessed by NeuN (red) colocalization. DAPI (blue) = nuclear counterstain. Example colocalized cell indicated by arrowheads. **(b)** Quantification of $GFP^+/NeuN^+$ neurons ipsilateral and contralateral to injection side. **(c)** Quantification of total $GFP^+/NeuN^+$ neurons across entire slice. n=5 mice per vector. n=12 random quadrants per side. Error bars = S.E.M. * $p < 0.05$. Scale bar = 20 μm.

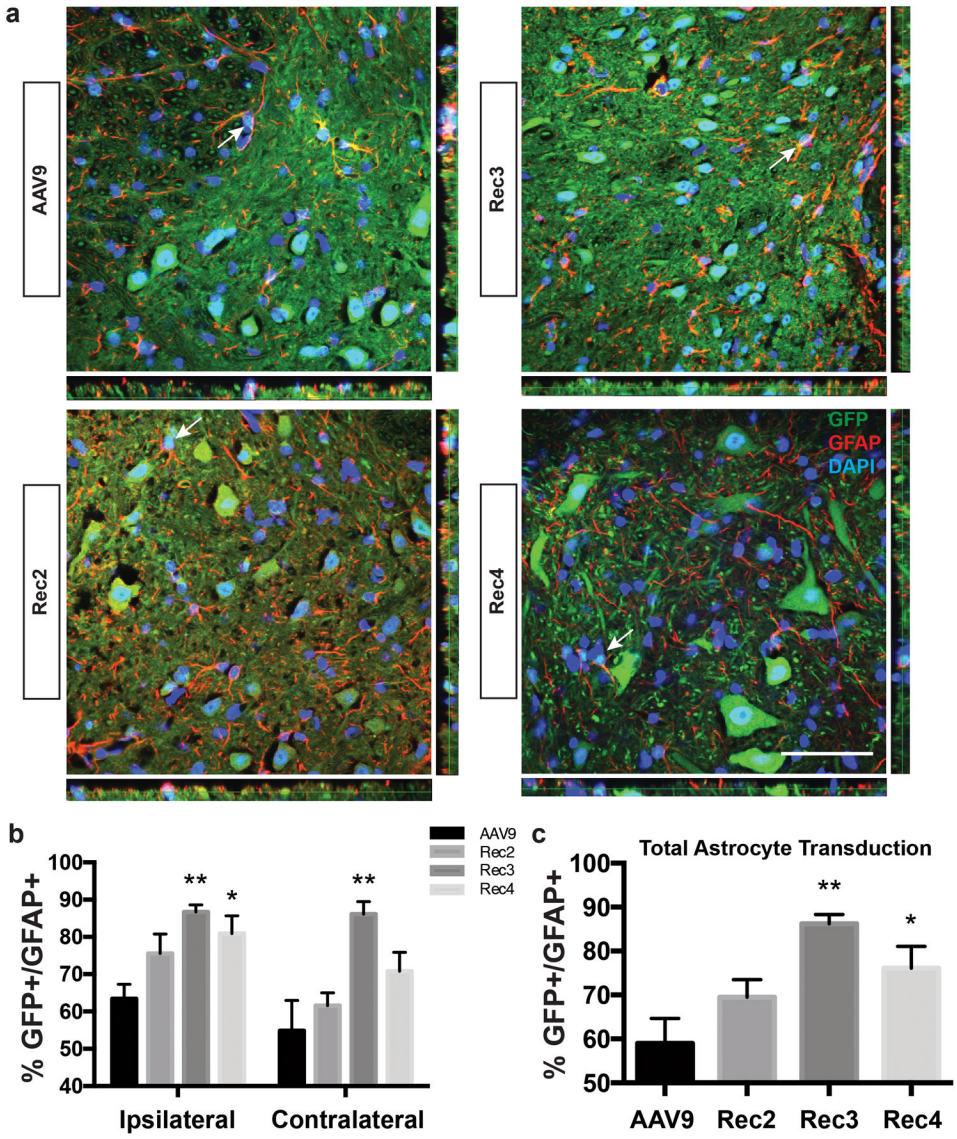

Figure 4. Comparison of astrocyte transduction by Rec vectors vs. AAV9

(a) Transduction (GFP, green) of astrocytes assessed by GFAP (red) colocalization. DAPI (blue) = nuclear counterstain. Example colocalized cell indicated by arrowheads. **(b)** Quantification of $GFP^+/GFAP^+$ neurons ipsilateral and contralateral to injection side. **(c)** Quantification of total $GFP^+/GFAP^+$ neurons across entire slice. n=5 mice per vector. n=12 random quadrants per side. Error bars = S.E.M. * $p < 0.05$. ** $p < 0.005$. Scale bar = 20 μm.

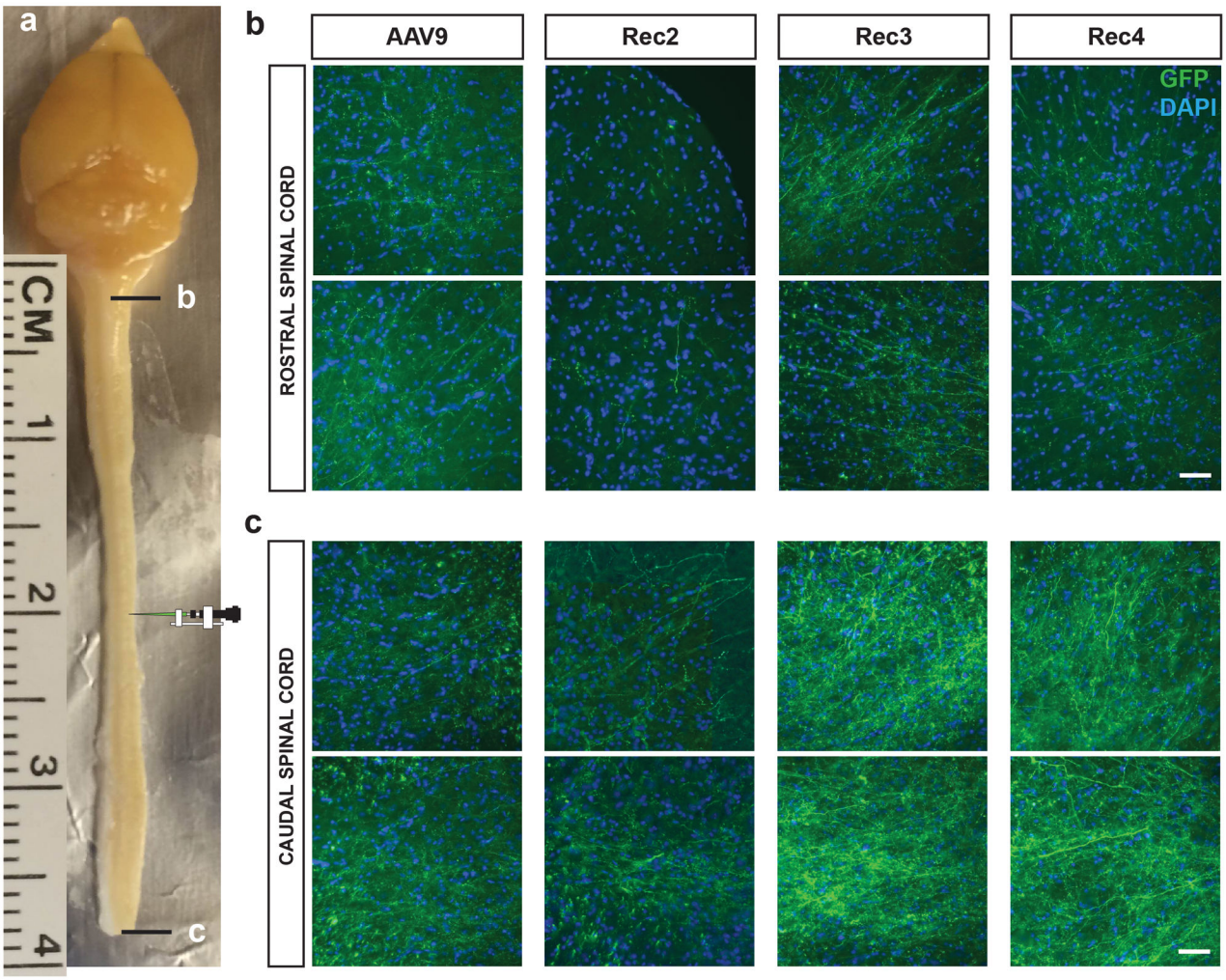

Figure 5. Anterograde & retrograde transport of GFP transgene protein in spinal cord

(a) Representative locations of rostral and caudal spinal cord images (b, c) relative to injection site at vertebral level T9. **(b)** Representative images of rostral spinal cord axons transduced with virus. **(c)** Representative images of caudal spinal cord axons transduced with vector. Scale bar = 100 μm.

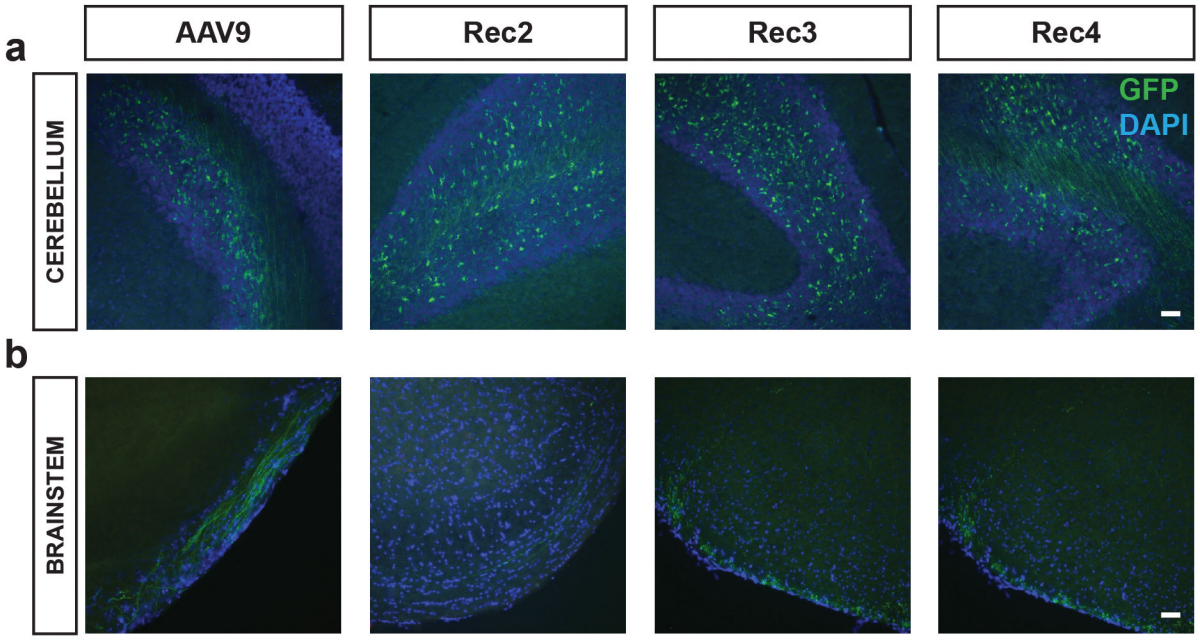

Figure 6. GFP distribution in brain after direct spinal cord gene transfer of AAV9 and Rec vectors

Representative images of CNS transduction in cerebellum **(a)** and brainstem **(b)**, assessed by GFP fluorescence in axonal fibers. Scale bar = 100 μm.

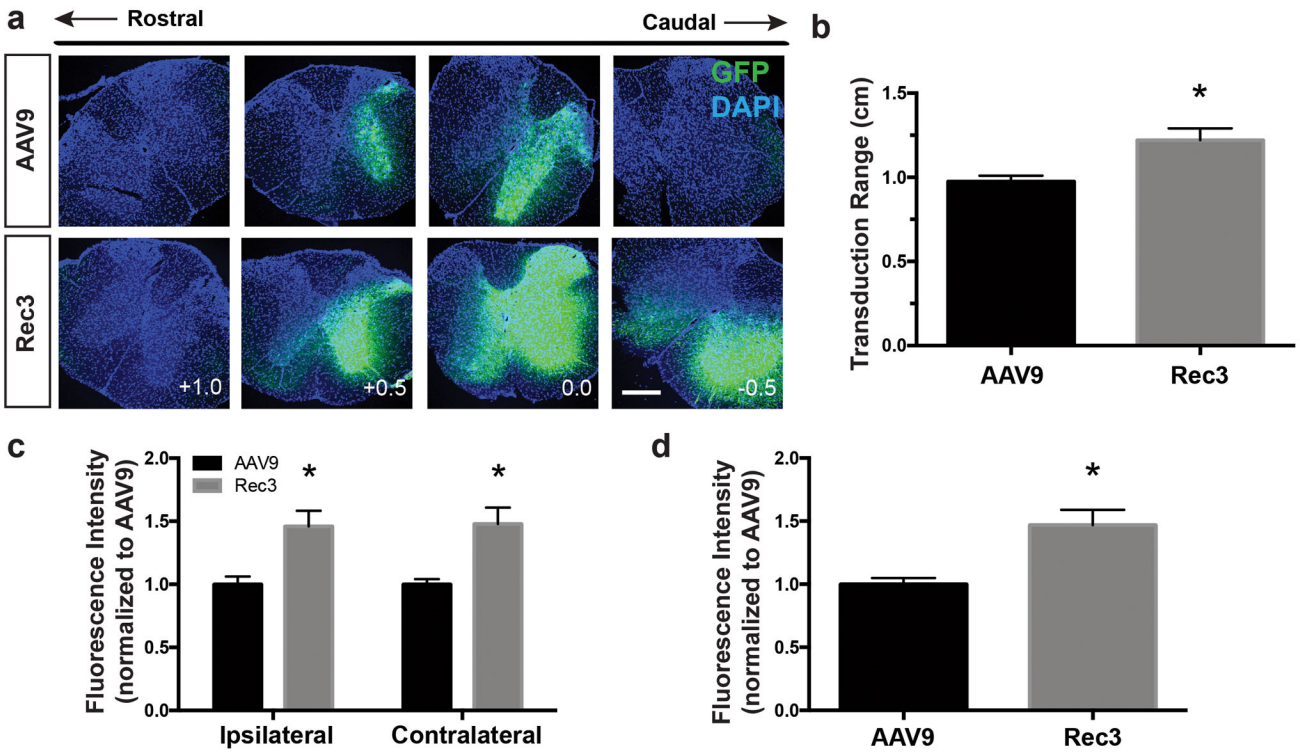

Figure 7. Longitudinal transduction range and transgene expression of Rec3 vs AAV9 serotypes at a 5-fold lower viral dose

(a) Representative images of GFP transgene expression along spinal cord. **(b)** Quantification of longitudinal transduction range in cm. **(c)** Quantification of GFP intensity ipsilateral and contralateral to side of injection. **(d)** Quantification of total GFP intensity across whole slice. n=5 mice per vector. n=12 random quadrants per side. Error bars = S.E.M. * = $p < 0.05$. Scale bar = 500 μm.

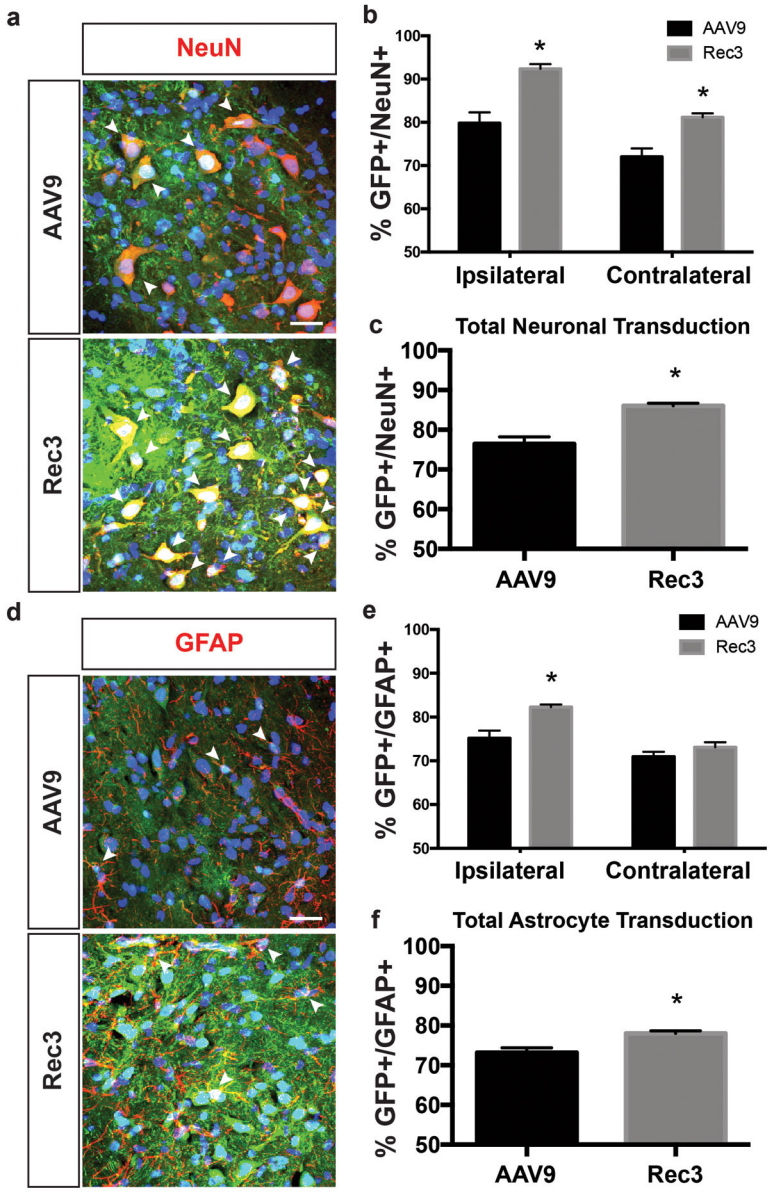

Figure 8. Comparison of neuronal and astrocyte transduction by Rec3 vs. AAV9 serotypes at a lower viral dose

(a) Transduction (GFP, green) of neurons assessed by NeuN (red) colocalization. DAPI (blue) = nuclear counterstain. Example colocalized cells indicated by arrowheads. **(b)** Quantification of $GFP^+/NeuN^+$ neurons ipsilateral and contralateral to injection side. **(c)** Quantification of total $GFP^+/NeuN^+$ neurons across entire slice. **(d)** Transduction of astrocyts assessed by GFAP (red) colocalization. Example colocalized cells indicated by arrowheads. **(e)** Quantification of $GFP^+/GFAP^+$ neurons ipsilateral and contralateral to injection side. **(f)** Quantification of total $GFP^+/GFAP^+$ neurons across entire slice. n=5 mice per vector. n=12 random quadrants per side. Error bars = S.E.M. * $p < 0.05$. Scale bar = 20 μm.